Effect of oxygen impurities on the critical properties of the (2 × 2)-2H/Ni(111) order-disorder phase transition

K. Budde, L. Schwenger,* C. Voges, and H. Pfnür
Institut für Festkörperphysik, Universität Hannover, Appelstraße 2, D-30167 Hannover, Germany
(Received 8 February 1995)

Critical behavior of the two-dimensional order-disorder phase transition of the (2×2)-2H structure on Ni(111) was studied by high-resolution low-energy electron-diffraction experiments, both for the pure system and with atomic oxygen, at concentrations between 0.3% and 3% of a monolayer added as an impurity. By quantitative profile analysis of several superstructure spots as a function of temperature the critical exponents β, γ, and ν were determined over a range in the reduced temperature, $t = (T - T_c)/T_c$, between 0.001 and 0.1. At smaller values of $|t|$ the system is finite-size limited. Crossover between four-state Potts behavior further away from T_c and exponents close to those of the two-dimensional Ising class were found. The crossover temperature depends systematically on the concentration of oxygen. We conclude that oxygen atoms seem to act like quenched impurities on this surface, similar to local defects already present at concentrations of $\leq 10^{-3}$ of a monolayer on the clean surface.

I. INTRODUCTION

Although phase transitions and critical phenomena in two dimensions (2D) have attracted wide interest in the past,[1–3] there is a surprising gap between experimental realizations and the wealth of theoretical investigations and modeling. Low-dimensional systems are interesting, because fluctuations play a much more important role than in 3D, so that large deviations from mean field behavior are observed. From the experimental point of view, investigations of superstructures formed by adsorbed atoms or molecules and of their often continuous order-disorder phase transitions are very attractive, because they give access to basically all universality classes that can be experimentally reached in 2D.[4] In particular, order-disorder phase transitions in the three- and four-state Potts universality classes can be and have been successfully studied.[5,6]

One of the main problems in these experimental studies is defects and impurities. In most experimental systems, the concentration of steps and point defects of the clean surface can hardly be reduced below the level of 0.1%, or, at least, it cannot be controlled. In the simplest case, finite-size effects are observed, i.e., long-range order and also correlations of critical fluctuations are disrupted by extended defects like steps. This limits the range over which critical behavior can be observed. In more complex situations, e.g., if coupling of fluctuations across steps occurs, many terraces have to be considered as one system close to T_c, which has a lower symmetry than the flat surface. Corresponding changes of critical exponents should be expected, and have actually been observed for O/Ru(0001)-$p(2 \times 2)$.[7,8]

The role of a random distribution of frozen point defects has been studied in a variety of spin models,[9–12] which, however, can only be partially mapped onto adsorbate systems. Random quenched point defects either produce a random field or a random bond effect. Whereas the random field affects different sublattices (or spin orientations) differently, random bonds do not discriminate between sublattices. An arbitrary small random field is predicted to destroy long-range order.[9,13,14] In contrast, for a system containing a random quenched distribution of broken bonds, new stable critical points are predicted with altered critical exponents in case that $\alpha > 0$, where α is the critical exponent of the specific heat.[15] The phase transition should remain unchanged for $\alpha \leq 0$. These predictions are corroborated by extended studies of the limiting case of the 2D Ising model ($\alpha = 0$).[10–12] Monte Carlo studies of the Baxter[16] and Baxter-Wu models[17] with random quenched site impurities (both having $\alpha > 0$ for the pure systems) indeed show dramatic changes of critical exponents for the impure systems. Site disorder in fact combines aspects of random field and random bond impurities, similar to the situation for adsorbed layers containing impurities. Systematic experimental studies of the role of this type of defect, in other universality classes than the Ising class,[18–20] in particular in the three- and four-state Potts classes, are still missing.

In our experimental study of the critical properties of the order-disorder phase transition of the (2 × 2) structure of atomic H on the Ni(111) surface, described below, we tried to explore the effect of local defects, which are so strongly bound to the surface (in comparison with hydrogen) that they may act essentially as quenched defects. For this purpose, we added small concentrations of atomic oxygen to the hydrogen layer.

The phase diagram and the geometric structure of H in the ordered state are well known.[21] At surface temperatures above 100 K, the (2 × 2)-2H honeycomb structure (see Fig. 1) is the only ordered phase of adsorbed hydrogen, with a coverage of 0.5 ML for the completed structure. Both threefold coordinated (fcc and hcp) sites are occupied.[21] According to the Landau rules,[4] the order-

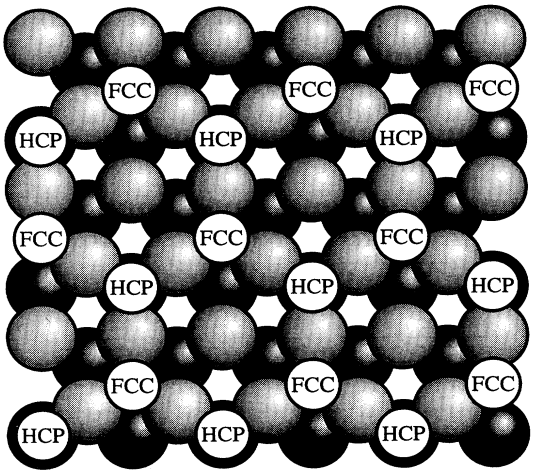

FIG. 1. Hard sphere model of the (2×2)-2H/Ni(111) structure at half monolayer coverage. Both fcc and hcp threefold sites are occupied with equal probability.

disorder phase transition of this structure is expected to fall into the four-state Potts universality class, if the transition is continuous. Pure oxygen, on the other hand, is known to occupy only the fcc site at low coverage.[22] In an H-O mixture part of the hydrogen sites are blocked by oxygen, no matter whether adsorption of oxygen still takes place on the same sites as in the pure layer or oxygen atoms are shifted to the other three-fold site. Bond energies are also expected to change because the interaction between H and O should be different from the H-H interaction. Therefore, apart from the "field" effect due to blocking of sites of a certain hydrogen sublattice, there is also a bond effect, because the interactions on all neighboring sites of an oxygen atom both between O-H and H-H can be expected to be modified.

At the temperatures relevant for our investigation (240–300 K) and at the oxygen coverages used (0.003–0.03 ML), the pure oxygen system is above the ordering phase transition[23] of the coexistence between $p(2\times2)$ islands and disordered $2d$ gas. The formation of $p(2\times2)$ islands at low coverage indicates that there is an attractive interaction between the O atoms for this distance, which will cause a tendency for small cluster formation at temperatures even considerably above the phase transition mentioned. This cluster formation seems to survive hydrogen coadsorption, as shown below. The form of the phase diagram at low coverage[23] suggests that true equilibrium might not have been reached at coverages below 0.05 even for the pure oxygen system, because of very slow ordering kinetics, indicating considerable, although not quantifiable, activation barriers for diffusion of oxygen atoms on this surface. In contrast, hydrogen does not order at coverages below 0.4 and at temperatures above 200 K. The necessary exchange with hydrogen, i.e., the correlated motion of both H and O for oxygen to diffuse, will further reduce mobility of oxygen atoms. Because of the low mobility of these (otherwise disordered) clusters of O atoms, which might also contain some H atoms after adsorption of half a monolayer of H, they might not equilibrate with the surrounding pure H layer in the typical time of measurements (30–60 min). For this reason, they can act as quenched impurities in the H layer. In this study, we try to quantify the influences of this type of impurities on the critical properties of the (2×2)-2H order-disorder phase transition. A preliminary short report of this study was published recently.[24]

II. EXPERIMENTAL AND NUMERICAL PROCEDURES

We carried out our experiments in a μ-metal shielded UHV chamber at a base pressure of 3×10^{-9} Pa. The sample, a nickel-disk of ≈ 20 mm in diameter and 3 mm thick, was cut from a single crystal rod by spark erosion and etched on both sides in order to remove the layers damaged by the cutting process. The surface was then oriented to within 0.02° of the (111) direction, and polished with diamond pastes from 15 μm grain size down to 0.25 μm in several steps. Chemomechanical steps in between seemed to improve the final quality of the crystal surface.

The surface was first cleaned by extensive Ar^+ sputtering (750 eV, 5 μA) at room temperature until no impurity could be detected by Auger electron spectroscopy. In further sputter cycles the crystal temperature was held at 560 K in order to remove carbon dissolved in surface-near bulk regions: At this temperature bulk carbon has a large mobility and a small solubility within the crystal, so that it migrates to the surface.[25] Only when no carbon was detectable, the crystal was annealed for 2 min at 1000 K. Sputtering cycles were continued routinely long after no carbon was detectable any more. The clean surface used for the measurements presented here had an average terrace width of roughly 700 Å, as measured by low-energy electron diffraction (LEED) profile analysis.

The LEED measurements were carried out by means of a high-resolution instrument [SPA-LEED (Ref. 26)] with an effective transfer width of 1200 Å. The sample could be cooled to 95 K with lN_2 and heated to 1400 K by electron bombardment. During measurements only radiation heating was used. A NiCr-Ni thermocouple was spot welded to the rim of the crystal, which allowed us to measure and stabilize the sample temperature with a resolution of 0.01 K.

H and O (99.999% pure) were dosed to the sample from a capillary array. Exposures through the effusion system, were reproducible to within 0.5%. Oxygen was always preadsorbed at a sample temperature of 400 K after annealing the sputtered surface. Absolute oxygen coverages were evaluated assuming that the maximum in T_c of the $p(2\times2)$ structure, investigated previously in the same vacuum chamber,[27] corresponds to a coverage of 0.25, and that the sticking coefficient is constant up to this coverage. The latter assumption has been verified by our own measurements for $\Theta_{\mathrm{Oxygen}} \lesssim 0.24$ ML.[22]

Hydrogen was adsorbed at 290 K *after* oxygen deposition. As the hydrogen exposure necessary to reach the maximum transition temperature of the (2×2)-2H structure turned out to be slightly dependent on the amount of

preadsorbed oxygen, preexperiments were carried out in order to find these exposures. Thus, we were able to reproduce these maxima to within ±0.5 K. Measurements were started right at T_c, and the temperature difference with respect to T_c successively increased in order to minimize the effects of continuous hydrogen adsorption from the background gas, which causes slow variation of coverage and T_c. During a set of measurements within 5 K of T_c, we only allowed a variation of T_c of less than 0.1 K. For a maximal change in T_c of 0.3 K, the measuring time on the same layer was limited to about 30 min. All spot profiles were measured in two perpendicular directions in **k** space at each temperature. Scans of peak intensity versus temperature were routinely taken between the profile measurements in order to ensure that T_c did not change. In Fig. 2, a typical scan of peak intensity of a superstructure spot versus temperature is shown. T_c was taken as the point of inflection in these curves. This point should coincide with the critical point of a continuous phase transition for any instrument with finite resolution, which effectively integrates over fluctuations close to T_c.[28] From the minimum in the derivative of the data with respect to T, it was possible to determine the critical temperature to within ±0.2 K [see also Fig. 2(b)]. T_c was redetermined for each measurement and used to evaluate reduced temperature.

First and second order superstructure spot profiles were measured and analyzed in the radial direction, with respect to the (00) spot and in the corresponding perpendicular direction. For data analysis, three contributions to the idealized spot profiles were taken into account according to the following parametrization:[29]

$$S(\mathbf{q}_{\parallel},t)=\underbrace{I_0(t)\delta(\mathbf{q}-\mathbf{q}_0)_{\parallel}}_{\text{(i)}}+\underbrace{\frac{\chi_0(t)}{1+(\mathbf{q}-\mathbf{q}_0)_{\parallel}^2\xi^2(t)}}_{\text{(ii)}}+\text{bg}\ . \tag{1}$$

Term (i) describes the contribution from the *long-range order*. For a continuous phase transition, it behaves like

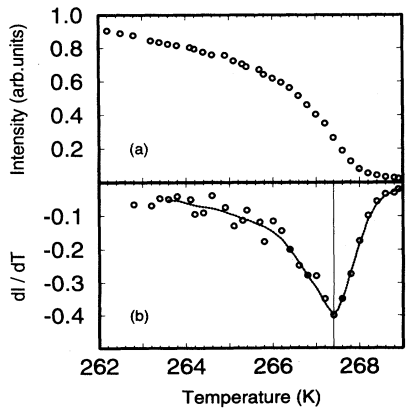

FIG. 2. Typical scan of spot intensity $S(\mathbf{q}_{\parallel}=\mathbf{q}_0,T)$ of a superstructure spot versus temperature (a). The derivative of (a) is shown (b). The minimum in (b) is used to estimate T_c.

$I_0 \propto |t|^{2\beta}$ for $T < T_c$, where $t=\frac{T-T_c}{T_c}$ is the reduced temperature and β the critical exponent of the order parameter Φ ($\Phi \propto \sqrt{I_0} \propto |t|^{\beta}$) . For $T > T_c$, $I_0 = 0$. $\mathbf{q}_0$ denotes a reciprocal lattice vector of the superstructure. Term (ii) describes the contribution of short-range fluctuations of the order parameter (critical scattering). This term is most easily measured above T_c because it is the only remaining term, apart from the background, bg, which was also fitted. χ_0 denotes the susceptibility and ξ the correlation length. For a second order phase transition, they behave like $\chi_0 \propto |t|^{-\gamma}$ and $\xi \propto |t|^{-\nu}$.

Measured profiles always consist of two-dimensional convolutions of an ideal profile [Eq. (1)] and the instrumental transfer function. Because of numerical stability, we carried out numerical fits to the experimental profiles instead of trying to deconvolute them. A low temperature experimental profile of the superstructure beam was used as the instrumental function in the scan direction, whereas in the perpendicular direction, it was approximated by a Gaussian. More sophisticated procedures were tested, but turned out to have little to no influence on the values of critical exponents determined.

III. RESULTS

First and second order superstructure beam profiles were used for the analysis described below. A comparison of FWHM's (full width at half maximum) of the superstructure spots at a hydrogen coverage of $\Theta_H = 0.5$ ML and at a temperature far below T_c with those of integral order beams shows that the widths of the superstructure beams are constant as a function of electron energy and corresponds approximately to the width of integral order beams at an out-of-phase condition. We conclude, therefore, that long-range order of hydrogen is limited to one terrace, and no correlations between different terraces exist.

Contributions corresponding to the term (ii) in Eq. (1) could only be separated for $t > -0.0015$. This accessible range below T_c was too small to allow determination of critical exponents γ' and ν'. Therefore, all diagrams for χ_0 and ξ include only data points for $t > 0$. This finding is in agreement with simulations for continuous phase transitions in two dimensions. The (universal) amplitude ratios $\chi_0(t)^{t>0} : \chi_0(t)^{(t<0)}$ were found to be between 30:1 and 40:1 for two-dimensional systems, depending on the universality class of the system considered.[30,31] On the other hand, this also means that the peak intensities for $|t| > 10^{-3}$ below T_c are not influenced by contributions from critical scattering. Therefore, we tried to determine effective critical exponents from the raw data of peak intensities in this range of reduced temperatures. Log-log plots of these data are shown in Fig. 3 versus reduced temperature, with T_c determined as described above.

Even for the pure hydrogen layers, we do not find simple power law behavior. There are indications for leveling off in the reduced temperature range between 10^{-3} and 10^{-4}, more clearly seen in the data above T_c, which are most likely due to finite-size effects (see also the analysis of critical scattering below). The rest of the curve

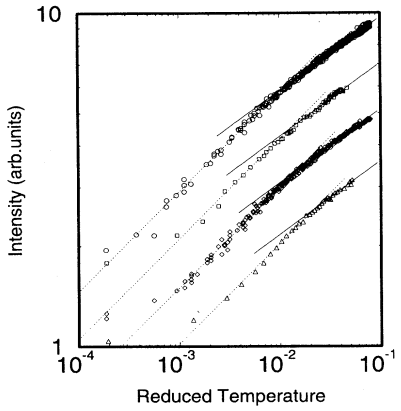

FIG. 3. Log-log plot of the peak intensity of superstructure beams as a function of reduced temperature below T_c for the (2 × 2)-2H/Ni(111) layer. The following amounts of oxygen were preadsorbed: clean surface (○), 0.3% (□), 1% (◇), 3% (△). Lines represent power law behavior with effective critical exponents $2\beta = 0.30$ for $|t| < 10^{-2}$ and $2\beta = 0.22$ for larger $|t|$. For clarity, the individual data sets are shifted against each other.

can be approximated by two straight lines, which cross at $t \simeq 10^{-2}$. The slopes, identified with effective critical exponents of the order parameter, 2β, obtained by this construction are $2\beta = 0.22$ for $|t| > 10^{-2}$, and $2\beta = 0.30$ below this value of $|t|$. This construction is only meaningful if indeed a crossover between two different regimes occurs, but contains some arbitrariness at the moment. However, as it turns out by analyzing the data above T_c, we obtain a similar behavior above T_c, if, as required for a continuous phase transition, the same T_c's are used for the analyses below and above T_c. Variation of T_c within the limit of experimental uncertainties does not allow description of the data by single power laws. Simple power law behavior could only be obtained by a systematic lowering of T_c for the data below T_c and a simultaneous increase of T_c for data above T_c, which is obviously not meaningful.

If a change of critical properties close to T_c occurs, it may be caused by impurities or other local defects on the surface. In order to test this idea, we performed a series of systematic studies using atomic oxygen as impurity, which, as mentioned, was always preadsorbed. Concentrations of preadsorbed oxygen between 0.003 and 0.03 ML were tested. H and O do not react on this surface in the temperature range of interest here, as explicitly demonstrated by the reversibility of all measurements. Oxygen preadsorption, however, has the effect of slightly lowering T_c (see Table I) and of systematically shifting the crossover point to higher reduced temperatures (see Fig. 3). It is interesting to note, that the lowest oxygen concentration tested yields essentially identical results as the pure hydrogen layer. The behavior above T_c for this oxygen concentration is consistent with this finding below T_c. We conclude that there must be defects or impurities present already on the clean surface, which act very much in the same way as the adsorbed oxygen atoms. Taking into account the tendency of oxygen to form small clusters in the temperature range investigated here (see below), the concentration of these defects must be of the order of 10^{-3} or below.

TABLE I. Changes of T_c as a function of oxygen preadsorption, and correlation lengths at crossover points.

Θ_{Oxygen} (ML)	T_c (K)	$\xi_{\text{cross over}}$ (Å)
0	267.2	~ 200
0.003	267.0	$\simeq 200$
0.01	265.5	$\simeq 100$
0.03	263.5	$\simeq 50$

The trends just described as a function of temperature and oxygen precoverage were found even more pronounced above T_c, so that a fully consistent picture is obtained. Only scattering from fluctuations remains in this temperature range. For these results, fitting of a convoluted function according to Eq. (1) is essential. Examples are shown in Fig. 4. In Figs. 5–7 we show the sequence of results for the (deconvoluted) amplitude of critical scattering and for the inverse half widths (taken as the correlation lengths), obtained as a function of increasing oxygen precoverage.

The data of the pure (2×2) layer and those with 0.003 ML of preadsorbed oxygen virtually coincide. Therefore, only the data set without preadsorbed oxygen is shown in Fig. 5.

Data from different orders of superstructure spots also coincide, as do data taken in different scan directions on the same spot. For $t < 10^{-3}$, a leveling off of both critical amplitudes and correlation lengths is found again. From the nearly temperature independent correlation lengths in this range of reduced temperatures, this leveling can be clearly identified as a finite-size effect. The value of ξ in this range of 700–1000 Å corresponds well to the average terrace size estimated above, and is consistent with the model of independent order on each terrace. If the data for $t > 10^{-3}$ are again approximated by two straight

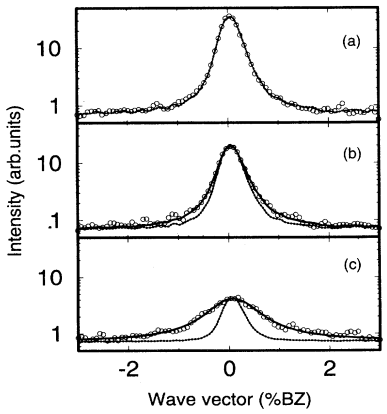

FIG. 4. Typical experimental profiles for $T_c - 0.5$ K (a), $T_c + 0.5$ K (b), and $T_c + 3$ K (c). Circles are data points, the dashed curves correspond to effective instrument functions, as determined from low temperature profiles. Full lines: fits according to Eq. (1). Amplitudes and inverse half widths are extracted from these fits.

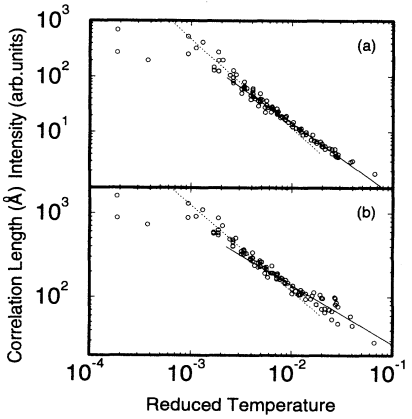

FIG. 5. Log-log plot of the amplitudes of critical scattering (a) and correlation lengths (b) for $t > 0$ in a pure H layer. Oxygen preadsorption of 0.003 ML produced virtually an identical result. Data of the first and second order superstructure beam are plotted together. Slopes of straight lines in (a) correspond to effective exponents of the critical amplitudes $\gamma = 1.65$ (dashed line) and $\gamma = 1.28$ (solid line). Slopes for correlation lengths yield effective exponents $\nu = 1.03$ and $\nu = 0.69$ (b).

lines, the data are best described by a crossover close to $t = 6 \times 10^{-3}$ and two sets of effective critical exponents. The values for $t > 6 \times 10^{-3}$ can be determined more reliably. Varying T_c and the crossover within the limits of uncertainty, we obtain $\gamma = 1.2 \pm 0.1$ and $\nu = 0.68 \pm 0.05$.

These values agree very well with those expected for a continuous phase transition in the four-state Potts universality class, i.e., for small values of the correlation lengths, we obtain the behavior expected for a pure system with this type of unit cell for the ordered layer. Although the measured critical exponent for the order parameter of 0.11 is somewhat larger than expected

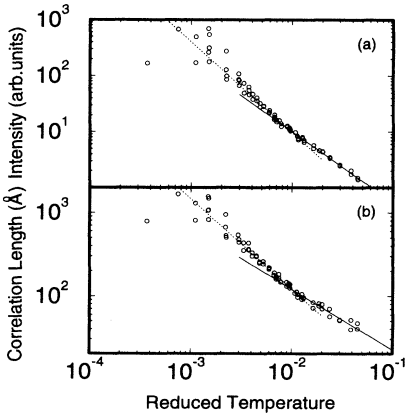

FIG. 6. Same as Fig. 5, but with 1% of a monolayer of preadsorbed atomic oxygen. The straight lines drawn into the data correspond to effective critical exponents $\gamma = 1.78$ close to T_c, $\gamma = 1.20$ further away from T_c. The corresponding values for ν are $\nu = 1.03$ and $\nu = 0.65$, respectively.

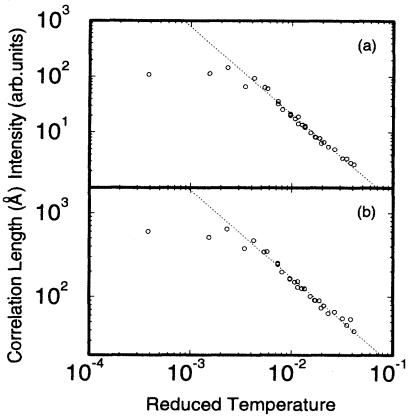

FIG. 7. Same as Fig. 5, but with 3% of a monolayer of preadsorbed atomic oxygen. The straight lines drawn into the data correspond to effective critical exponents $\gamma = 1.63$ and $\nu = 1.01$.

($\beta = 0.083$ for the four-state Potts universality class[32]), scaling laws are well fulfilled by these exponents within experimental uncertainties. The large value of β might be an indication that logarithmic corrections to scaling[33] play some role in this system, which were found not to be important in systems within the same universality class studied earlier.[5,6,34] This change in behavior may not be totally unexpected, as the local structure differs [honeycomb (2×2) versus $p(2 \times 2)$ in the earlier studies]. Our findings are in full agreement with a transfer matrix calculation for the simplest model able to produce a honeycomb (2×2) structure close to half monolayer coverage,[35] which not only found a continuous phase transition, but a value for the exponent ν slightly larger than the theoretical value of 2/3.

The effective exponents determined for the intermediate range of reduced temperatures $1 \times 10^{-3} < t < 6 \times 10^{-3}$ are $\gamma = 1.7 \pm 0.2$ and $\nu = 1.0 \pm 0.1$. The larger error bars are simply due to the shorter range of reduced temperature available in this case. Within uncertainties, however, the effective critical exponents determined here coincide with those of the measurements at the highest oxygen concentration of 3% of a monolayer (see Fig. 7). Here, the crossover is barely visible any more, in agreement with the data below T_c, which extended to larger $|t|$ with smaller scatter of data. The data of critical scattering at 3% oxygen precoverage, apart from the finite-size dominated temperature range, can be described by single exponents of $\gamma = 1.68 \pm 0.15$ and $\nu = 1.03 \pm 0.08$, respectively.

For the intermediate oxygen precoverage of 0.01 ML (Fig. 6), the shift of the crossover point compared to smaller oxygen concentrations can be seen. The effective critical exponents determined for this oxygen concentration are fully compatible with the values just given. The results of our experiments are summarized in Table II. It shows that the effective critical exponents of those parts dominated by the influence of the impurities are close to those of the Ising universality class.

IV. DISCUSSION

In this study, we were able to demonstrate the crucial role of defects for the critical behavior of an order-disorder phase transition in two dimensions. Although strong influences of defects and impurities were found even on a surface as perfect as possible, the (2×2)-2H order-disorder phase transition is not totally dominated by defects. In the temperature range above $|t| > 6 \times 10^{-3}$ on this nominally clean surface, we were still able to identify effective critical exponents close to those of the four-state Potts universality class. Since for the exponents γ and ν, in particular, corrections to scaling do not seem to be very important in adsorbed layers belonging to this universality class, so that reliable identification of these exponents was still possible experimentally in the systems O and S on Ru(0001) in a comparable range of reduced temperatures,[5,6] we are confident that the order-disorder phase transition of the pure (2×2)-2H structure on Ni(111) investigated here is again continuous.

Defects on this surface have several effects. First, the line defects of the terrace structure of the surface seem to interrupt long-range order, as seen both from the widths of superstructure spot profiles far below T_c, and from the limits of the correlation lengths, causing a typical finite-size effect. Point defects on the other hand, either those already present on the clean surface or induced by the added oxygen atoms, lead to the behavior shown in Figs. 3–7. It can consistently be described by two sets of effective critical exponents, apart from the range $|t| < 10^{-3}$, which is dominated by finite-size effects. We would like to stress that this analysis would be far from being unique, if carried out at only a single impurity concentration.

A crucial point in the discussion of our results is the question of residual mobility of the oxygen impurities. If they are frozen in—at least on the time scale of our experiments—they are not in thermodynamic equilibrium with the surrounding hydrogen layer close to the critical point of the (2×2)-2H transition, and should produce a behavior different from that of mobile impurities, which eventually should equilibrate. Impurities at thermodynamic equilibrium have an effect similar to vacancies, i.e., the dependence of the chemical potential on coverage, which is absent at the symmetry point of the phase diagram of the clean system, becomes important again close to T_c, and should lead to Fisher renormalization of the critical exponents[36] close to $t = 0$, with a crossover to the nonrenormalized exponents further away from T_c. This behavior in the impure system can even occur at the point of maximal T_c, with respect to the hydrogen concentration, since the concentration of impurities is fixed in the experiment. Fisher renormalization could lead to a behavior which is roughly similar to that observed. In case of a four-state Potts system, critical exponents should change from their ideal four-Potts value to a value three times larger close to T_c: e.g., $\beta \to \frac{\beta}{1-\alpha} = 3\beta$ (α also changes sign). As seen from our data, however, all changes in effective critical exponents are smaller than a factor 1.5. The effect of Fisher renormalization could still be hidden by effective crossover to the nonrenormalized exponents at small oxygen concentrations. If the increase in slope close to T_c were due to Fisher renormalization, its influence should increase as a function of oxygen concentration. Thus, it should have become most obvious at the highest concentration of oxygen. The data close to T_c, however, can be well described by the same effective critical exponents for all data sets without any indication for an increase at higher oxygen concentrations. Therefore, we conclude that the behavior found is not consistent with Fisher renormalization.

In qualitative agreement with Harris' predictions for (frozen) random bond disorder,[15] we see a widening of the defect-influenced region around T_c. For a quantitative test of the predicted concentration dependence x ($\Delta t \sim x^{1/\alpha}$), however, more data and a wider range of accessible reduced temperatures would be needed. Data can consistently be described by values of $\gamma = 1.68 \pm 0.15$ and $\nu = 1.03 \pm 0.08$ for the intervals in reduced temperature including the highest slope of data. While these values are very close to those expected for the Ising-universality class (see Table II), it is unclear at the moment, whether a true fixed point in the Ising class exists for the impure system. It is remarkable, however, that in the few simulational studies carried out in systems with random quenched impurities not belonging to the Ising-universality class,[16,17,37,38] i.e., for models with $\alpha > 0$, Ising-like exponents were obtained in all cases for the impure systems. These studies included random site disorder in the Baxter[16] and Baxter-Wu models,[17,37] which both have continuous phase transitions. The latter is particularly interesting in our context, because the pure system also falls into the four-state Potts universality class, although our lattice gas type system cannot be mapped on this model. The first order phase transition of the eight-state Potts model was shown to be converted to a continuous transition by random bond impurities, in agreement with a scaling argument by Berker.[39] Again,

TABLE II. Averages of experimentally determined effective critical exponents and comparison with theoretical expectations for the four-state Potts and the Ising universality classes.[a] "Pure" means exponents determined from those sections of the experimental data not influenced by the oxygen impurities. Exponents from the impurity dominated parts are labeled "impure."

	Experiment		Theory	
	pure	impure	Ising	four-state Potts
β	0.11±0.02	0.15±0.02	0.125	0.083
γ	1.23±0.1	1.68±0.15	1.75	1.167
ν	0.68±0.05	1.03±0.08	1.0	0.667

[a]See Ref. 32.

critical exponents of the Ising class were found.[38]

As mentioned in the Introduction, both random field and random bond effects may play a role in the context of our experimental system. Our results show that both crossover and long-range order up to the system (= terrace) size can still be observed in the defect dominated range of reduced temperatures. A pure random bond effect seems to be highly unlikely as an explanation for this behavior. The adsorption of oxygen on fcc sites breaks symmetry in the sense that, due to the modified interaction of oxygen with the four honeycomb sublattices of hydrogen, it divides the sublattices into two sets. The three sublattices, to which the site directly blocked by oxygen does not belong, are symmetrically equivalent with respect to oxygen on an fcc site and form one set, the remaining sublattice forms the other. Regarding this random field contribution, the average distance between the defects is evidently not the length scale on which long-range order or critical fluctuations are destroyed. Long-range order might still be destroyed by the random field on a length scale larger than or close to our experimental system size, which is limited to one terrace width. The tendency of the finite size limited value of the correlation length to decrease with increasing impurity concentration could be an indication for the breakdown of critical fluctuations caused by the random field; the trend is not very conclusive, given the large error bars.

The role of impurities in this system is rather subtle and not fully understood at this moment. Obviously, the pure system already contains local defects, which affect the critical exponents close to T_c in very much the same way as the added oxygen atoms. These local defects are most likely either vacancies or other impurities like carbon atoms or clusters left over after the cleaning process. Especially vacancies cannot be mobile at the temperatures used in this study. They might also bind oxygen more strongly than the flat surface, so that small concentrations of oxygen atoms are preferentially adsorbed at these defects already present on the surface. Note that oxygen preadsorption was carried out at 400 K, where small concentrations of oxygen are most likely mobile. Thus, no additional defects are created at the smallest concentration of oxygen investigated, and the phase transition remains unchanged by this amount of oxygen. It naturally explains the low mobility of both the local defects just mentioned and of the oxygen atoms at very small concentrations.

The fact that oxygen forms clusters can be easily seen from the correlation lengths at the crossover points, which are far above the average separation of randomly distributed single oxygen atoms. Our parametrization of the correlation length does not necessarily yield the actual correlation length, so that we cannot determine the actual average cluster size of oxygen clusters. It is unlikely, however, that the actual correlation length is so much smaller that it would agree with the value expected for single impurity atoms. We, therefore, conclude that small oxygen clusters are formed within the (2×2)-2H layer. Clusters will certainly be less mobile than single impurity atoms, so that the clusters can act as effectively frozen impurities. Assuming that the interactions between oxygen atoms are similar for the pure and the hydrogen covered surface, (2×2) correlations prevail in these clusters so that symmetry considerations are the same for single oxygen atoms and clusters with respect to the (2×2) honeycomb lattice of hydrogen.

Summarizing, we have found that the order-disorder phase transition of the (2×2)-2H structure on Ni(111) is continuous, and yields critical exponents for the pure layers that are compatible with those of the four-state Potts universality class. Critical exponents are modified in the same way by point defects already present on the bare surface and by small amounts of preadsorbed oxygen. The range, in which modified critical exponents are observed, widens with increasing oxygen concentration. These findings suggest that both the defects on the bare surface and small clusters of oxygen atoms act as random quenched impurities within the hydrogen layer. These effects can be separated from those of extended defects like steps, which lead to finite-size rounding.

ACKNOWLEDGMENTS

Helpful discussions with T. L. Einstein, N. C. Bartelt, M. E. Fisher, and I. Lyuksyutov are gratefully acknowledged. One of us (H.P.) would also like to thank the members of the Physics Department of the University of Maryland at College Park for their hospitality while preparing this manuscript. This work was supported by the Deutsche Forschungsgemeinschaft.

* Present address: Centre d'Études Nucléaires de Saclay, DECRAM/SRSIM, 91191 Gif-sur-Yvette Cedex, France.

[1] E. Bauer, in *Structure and Dynamics of Surfaces II*, edited by W. Schommers and P. von Blanckenhagen, Topics in Current Physics Vol. 43 (Springer, Berlin, Heidelberg, 1987), p. 115.

[2] K. Binder and D. P. Landau, in *Molecule-Surface Interaction*, edited by K. Lawley (Wiley, New York, 1989), p. 91.

[3] B. N. J. Persson, Surf. Sci. Rep. **15**, 1 (1992).

[4] M. Schick, Prog. Surf. Sci. **11**, 245 (1981).

[5] H. Pfnür and P. Piercy, Phys. Rev. B **40**, 2515 (1989).

[6] M. Sokolowski and H. Pfnür, Phys. Rev. B **49**, 7716 (1994).

[7] M. Sokolowski and H. Pfnür, Phys. Rev. Lett. **63**, 183 (1989).

[8] M. Sokolowski, H. Pfnür, and M. Lindroos, Surf. Sci. **278**, 87 (1992).

[9] D. Blankschtein, Y. Shapir, and A. Aharony, Phys. Rev. B **29**, 1263 (1984).

[10] B. Shalaev, Phys. Rep. **23**, 131 (1994).

[11] J. S. Wang, W. Selke, V. L. Dotsenko, and V. B. Andreichenko, Physica **164**, 221 (1990).

[12] W. Selke, L. N. Shchur, and A. L. Talapov, in *Annual Reviews of Computational Physics*, edited by D. Stauffer

(World Scientific, Singapore, 1994).
[13] W. Kinzel, Phys. Rev. B **27**, 5819 (1983).
[14] L. D. Roelofs, Appl. Surf. Sci. **11/12**, 425 (1982).
[15] A. B. Harris, J. Phys. C **7**, 1671 (1974).
[16] D. Matthews-Morgan, D. P. Landau, and H. Swendsen, Phys. Rev. Lett. **53**, 679 (1984).
[17] M. A. Novotny and D. P. Landau, Phys. Rev. B **24**, 1568 (1981).
[18] H. Ikeda, M. Suzuki, and M. T. Hutchings, J. Phys. Soc. Jpn. **46**, 1153 (1979).
[19] I. B. Ferreira *et al.*, Phys. Rev. B **24**, 5192 (1983).
[20] M. Hagen, R. A. Cowley, R. M. Nicklow, and H. Ikeda, Phys. Rev. B **36**, 401 (1987).
[21] K. Christmann *et al.*, J. Chem. Phys. **70**, 5039 (1979).
[22] E. Schmidtke, C. Schwennicke, and H. Pfnür, Surf. Sci. **312**, 301 (1994).
[23] A. R. Kortan and R. L. Park, Phys. Rev. B **23**, 6340 (1981).
[24] L. Schwenger, K. Budde, C. Voges, and H. Pfnür, Phys. Rev. Lett. **73**, 296 (1994).
[25] T. Jach and J. C. Hamilton, Phys. Rev. B **26**, 3766 (1982).
[26] U. Scheithauer, G. Meyer, and M. Henzler, Surf. Sci. **168**, 441 (1986).
[27] L. Schwenger, C. Voges, M. Sokolowski, and H. Pfnür, Surf. Sci. **307–309**, 781 (1994).
[28] N. C. Bartelt, T. L. Einstein, and L. D. Roelofs, Phys. Rev. B **32**, 2993 (1985).
[29] H. E. Stanley, *Introduction to Phase Transitions and Critical Phenomena* (Oxford University Press, New York, 1971).
[30] V. Privman, P. C. Hohenberg, and A. Aharony, in *Phase Transitions and Critical Phenomena*, edited by C. Domb and J. L. Lebowitz (Academic Press, London, 1991), Vol. 14, p. 1.
[31] N. C. Bartelt, T. L. Einstein, and L. D. Roelofs, Phys. Rev. B **35**, 1776 (1987).
[32] F. Y. Wu, Rev. Mod. Phys. **54**, 235 (1982).
[33] J. L. Cardy, M. Nauenberg, and D. Scalapino, Phys. Rev. B **22**, 2560 (1980).
[34] P. Piercy and H. Pfnür, Phys. Rev. Lett. **59**, 1124 (1987).
[35] L. D. Roelofs, T. L. Einstein, N. C. Bartelt, and J. D. Shore, Surf. Sci. **176**, 295 (1986).
[36] M. E. Fisher, Phys. Rev. **176**, 257 (1968).
[37] M. A. Novotny and D. P. Landau, Phys. Rev. B **32**, 3112 (1985).
[38] S. Chen, A. M. Ferrenberg, and D. P. Landau, Phys. Rev. Lett. **69**, 1213 (1992).
[39] A. N. Berker, Physica A **194**, 72 (1993).

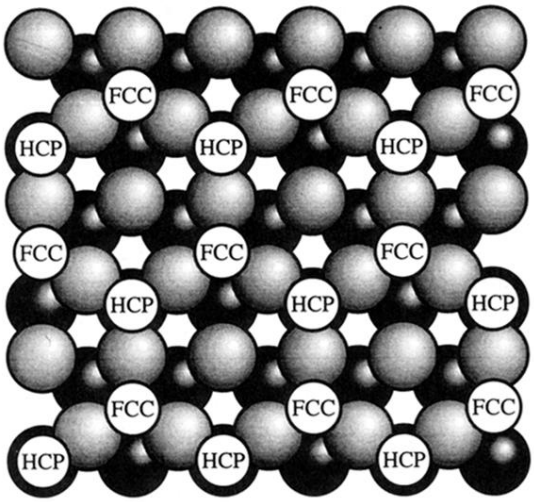

FIG. 1. Hard sphere model of the (2×2)-2H/Ni(111) structure at half monolayer coverage. Both fcc and hcp threefold sites are occupied with equal probability.